10th International Conference on Computer and Knowledge Engineering (ICCKE2020) October 29-30, 2020 – Ferdowsi University of Mashhad - Iran

An approach for enhancing hyperspectral change maps using morphological operations

Arash Azizi
Department of Electrical Engineering
Telecom. branch, Ferdowsi university of Mashhad
Mashhad, Iran
azizi.arash@mail.um.ac.ir

Amir Hossein Taherinia
Department of Computer Engineering
Ferdowsi university of Mashhad
Mashhad, Iran

***Abstract*— In this paper an enhancement method for hyperspectral change maps based on morphological operations is proposed in comparison to two common morphological operations. the effect of 2 initial thresholds was investigated and demonstrated. It is shown that this approach can perform better than or equal to two of common morphological operations via several indexes to demonstrate the efficiency of the proposed method including overall accuracy, F-Measure and etc.**

Keywords—Image processing, Remote sensing, Hyperspectral imagery, morphological operations

I. INTRODUCTION

In recent years remote sensing has drawn much interest from all disciplines such as agriculture, geology, urban management defense and intelligence; Due to its ability to detect resources, classify regions with different properties, monitor changes across timespans and etc…

Change detection refers to the detection of changes between two images collected at different times. There are a multitude of applications to change detection including: counting the number of ships in a dock, border monitoring where illegal activity may be detected, etc. there are some issues related to hyperspectral data such as non-optimal illumination, excessive cloud coverage, misregistration, parallax, etc. Due to the number of bands in hyperspectral and multispectral images, another important issue is computational load.

II. RELATED WORK

Some of the more traditional approaches for extracting change maps, include direct subtraction where two image cubes are subtracted element-wise [1], thresholded and then binarized. band ratios [2], which is resulted as the element-wise division of certain bands often followed by thresholding and binarizing. Principal component analysis (PCA) [3], which reduces the scarcity of information in multispectral or hyperspectral bands to only a few bands. In [4] a process called slow feature analysis will first obtain change residuals leading to a change map.

There have been some prediction based approaches like covariance equalization [5]. In this method both images are normalized, then their mean and covariance is calculated. As the next step eigenvalue decomposition is performed on covariance matrices and a transformation is suggested. Chronochrome (CC) method, similarly to CE, proposes a transformation however, there is no eigenvalue decomposition present. In [6] and [7] a standard two layer neural network is employed to derive a change map for hyperspectral or multispectral dataset.

In [8] Common morphological operations are successfully used to enhance binary images. In [9] opening and closing operations were employed to perform image processing tasks with a disk shaped structuring element. In [10] a small study was done on some morphological operations.

Morphological operation often need a structuring element. In [11] adaptive optimization of structuring elements of morphological filters in discrete spaces is studied. In image processing tasks the structuring element greatly affects the final result [10].

Some of more recent approaches utilize neural networks. In [12] a Convolutional neural network is proposed that extracts not only the spectral signatures but the spatial ones too. They have achieved a very high over all accuracy rate. In [13] a general end-to-end approach with a 2D CNN is used to derive a change map. An unsupervised deep noise modeling approach in [14] is used to obtain a change map.

A common issue when working with hyperspectral data is the noise mixed with signal caused by a variety of sources including atmospheric effects (such as dispersion), thermal noise, quantization noise, shot noise [15], pattern noise, sparse noise [16]... To counter the negative effects of noise, researchers have developed a multitude of approaches and methods that often denoise hyperspectral data as a preprocessing step. These methods span from using low pass filters [17] to residual convolutional neural networks [18]. In [19] a strategy is proposed to handle spatially-varying statistics cases such as changes of illumination.

In this paper a new approach for reducing the effect of noise in change detection applications is proposed as part of post processing.

III. METHODOLOGY

In order to test the enhancement technique, we will first need a method to derive a change map from two hyperspectral cubes taken at different times. For this purpose, we chose Percent difference (PD) method since our primary concern is to enhance the final change map.

There is a definition that's pivotal to the overall process. Therefore, it is explained first.

978-1-7281-8566-8/20/$31.00 ©2020 IEEE

A. Adjacency map

According to the definition of 4-adjacency, for each binary image each pixel is neighbor to 4 possibly different valued pixels. Adjacency map of a certain binary image is the matrix in which the value of each index is determined by how many of the corresponding pixel's neighbor are valued 0. The figures below are examples.

Only the points corresponding to white points in binary image will be non-zero. Indices in adjacency map corresponding to black points in binary image will be set zero.

Adjacency map resembles morphological gradient but is not binary. This map helps us identify certain pixels from change map.

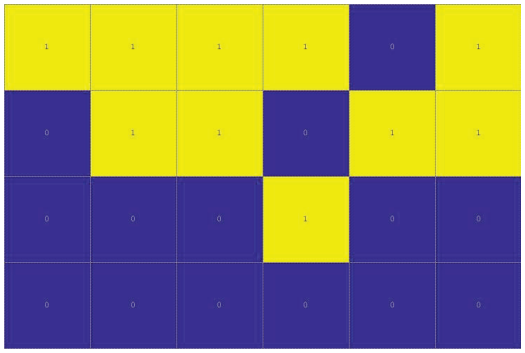

Figure 1: Binary image (Yellow = 1,Dark blue = 0)

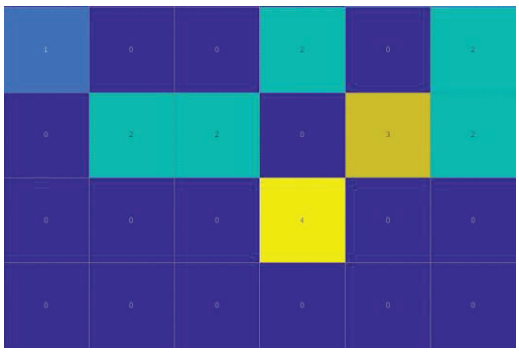

Figure 2: Adjacency map (Yellow = 4, Orange = 3, Cyan=2, Light blue = 1, Dark blue = 0)

B. Algorithms

There are two main algorithms that make up the overall process. It would be beneficial if they are explained in a modular manner. Both of them take a binary image as input and return one as output.

1) Algorithm 1: First of all, corresponding 3's of the change map are set to zero. Not to mention all of 4's are basically individual dots (most likely noise) and were already set to zero. In the second step, a certain percentage (r) of all 2's are set to zero. The optimal value of r is not the goal of this paper, but we decided to use 0.20. We found that greater percentages tend to deform changed areas and lesser values of *r* will slow the overall progress of the method.

2) Algorithm 2: First the image is inversed (if needed) in order to convert the changed areas to black. Then every white object is identified. Every object is then removed except when the object touches the borders of the image (thus part of the background).

The flowchart below demonstrates how these algorithms are used together.

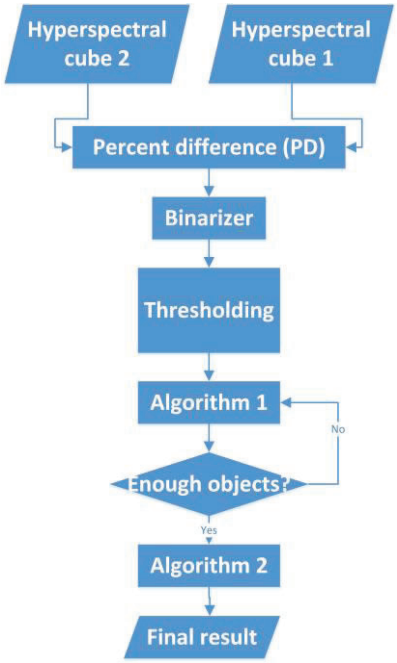

Figure 3: General flowchart

In the first step a cubic percent difference image is derived via direct subtraction and division. PD, HSI1, HSI2 are all cubic images of same size.

$$PD = \frac{HSI2 - HSI1}{HSI2} \quad (1)$$

Then each band is separately binarized with a threshold of *b*. Each band is treated as a single greyscale image.

In the next step, a 2D binary change map is produced as a result of collective thresholding between all bands of the binarized image. Only if over *p* percent of spectral values corresponding to a certain pixel are 1, then the result would be 1. Otherwise the corresponding pixel will be set to zero.

Algorithm 1 is performed on the binary change map returned from thresholding block.

Too many iterations on this step leads to deformation of changed areas and too few will cause missed areas. Thus an optimum number of iterations exist for each dataset. This number appears to be correlated with both of the thresholds used so far. We have determined this number to be 4 for both of datasets that will be introduced later.

Algorithm 2 removes the objects created by repetitive execution of algorithm 1 and creates an enhanced change map.

A complete analysis of the proposed method is done using every possible combination of *b* and *p* over the span of 0 to 1.

IV. Experimntal results

All simulations were done on a laptop equipped with intel core i5 2.53GHz, 6 GB of DDR3 RAM and AMD Mobility Radeon HD 5000 Series M, using MATLAB.

A. Datasets

Two pairs of change detection datasets were used in this simulation:

1) San Francisco dataset: The first one [20], a pair of multi-look quad-polarimetric UAVSAR airborne sensor in L-band with ground projection in WGS-84 and number of azimuth and range look is 12×3 that acquired over an urban area in San Francisco city (Figure 1) on 18- September-2009, and 11-May-2015, is used for the experiments. This dataset has 200×200 pixels and 138 bands [21].

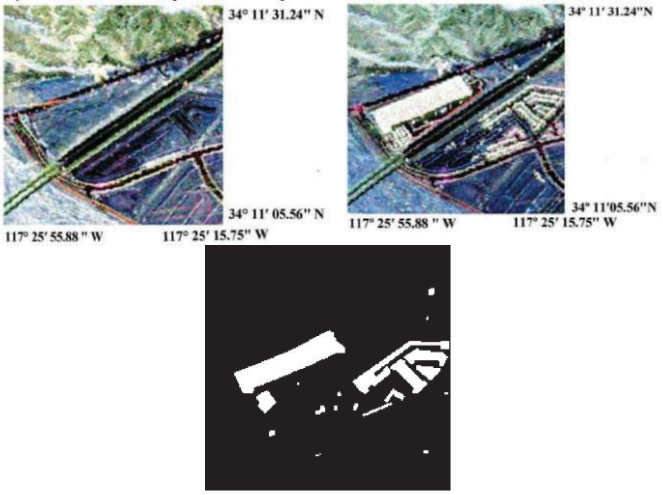

Figure 4: San Francisco dataset September 2009 - May 2015 –Ground truth

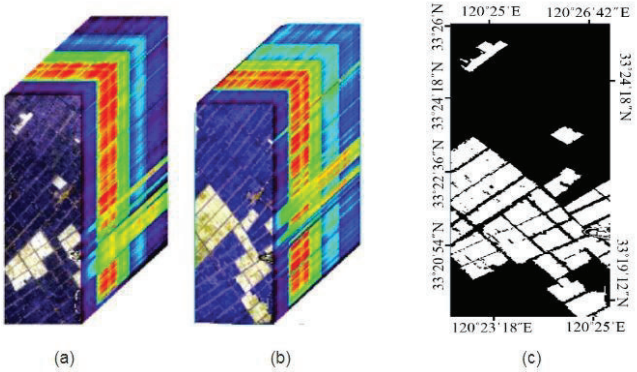

Figure 5: Yuncheng dataset May 3, 2006 and April 23, 2007

2) Yuncheng datasets: The other pair is taken at Yuncheng Jiangsu province in China in May 3, 2006 and April 23, 2007 has a scene size of 450x140 with 154 bands. This dataset was acquired using the hyperion sensor [22]. Both datasets were downloaded from [20] It should be that the raw change map resulting from the Yuncheng dataset was created using unity of two processes to detect changes of (b) (April 23, 2007) relative to (a) (May 3, 2006) *as well as (a) relative to (b).*

B. Results, comparison and discussion

In addition to qualitative comparison we will be using quantitative comparison using true positive, true negative, false positive and false negative indexes. However, they do not draw a complete picture of the overall performance. As a result, the indexes known as OA, OE, Kappa, Recall and FM [23] are used to gain better understanding.

Figure 6 shows the raw change map resulted by only using PD method of Dataset 1 using $b = 0.5$ and $p = 0.6$ and dataset 2 using $b = 0.03$ and $p = 0.2$. It should be noted that due to scaling of second dataset value of b was set smaller than that of first dataset.

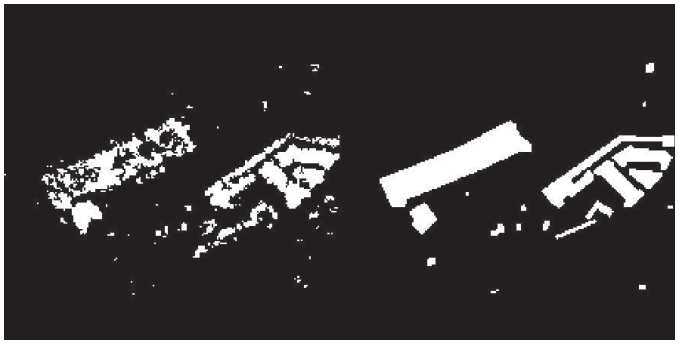

Figure 6: A) Dataset 1 raw change map – ground truth

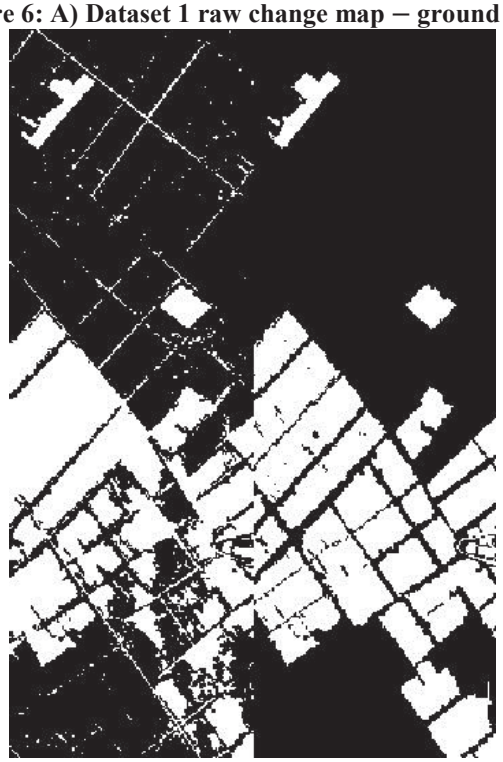

Figure 6: B) Dataset 2 raw change map – ground truth

To gain some insight about the procedure figure 7 shows changes of normalized TP, TN, FP, and FN and OA, OE, Kappa, Recall, FM across 10 iterations of the proposed method using the previous parameters.

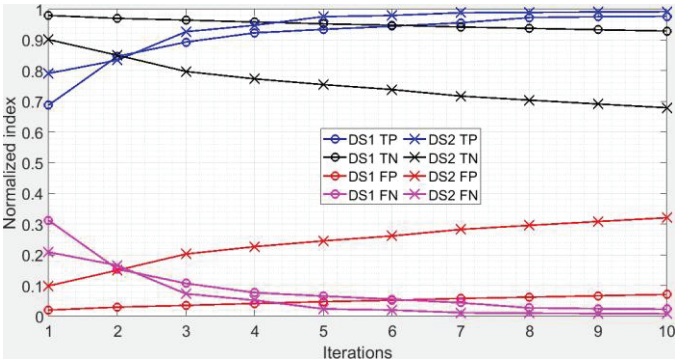

Figure 7: Normalized TP, TN, FP and FN values for 10 iterations

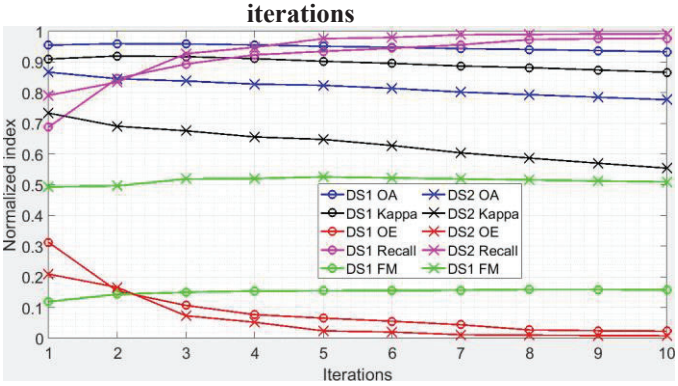

Figure 8: OA, Kappa, OE, Recall, FM values for 10 iterations

It is apparent from figure 7 that FP index indicates worse performance in Yuncheng rather than in San Francisco. This can be partially attributed to the fact that in dataset 1 changed areas are located in fair distance from each other but in dataset 2 this is not the case. Despite worse FP rates in dataset 2 we'll see that it leads to better overall performance. It seems the reason behind success of this method is exponential decrease of FN in spite of linear increase of FP over iterations.

Regarding figure 8 Overall accuracy increases in San Francisco dataset but decreases in Yuncheng dataset. Greater FP increase rate is primarily the cause. However, OA increase in Dataset 1 is not substantial. This is also the case for Kappa. Omission error (OE) decreases in both cases, with higher rate in dataset 1. As expected, recall increases in both cases. There is an interesting leap in second iteration of dataset 1 with respect to dataset 2. The behavior of FM is monotonic across all iterations in dataset 1 but this is not the case for dataset 2 as there is a maximum is sixth iteration. As the algorithm progresses to greater iterations, higher FP and lower TN will cause the overall accuracy and F-measure to decrease.

In the next step due to the large number of total outcomes we'll only demonstrate indexes of the first and fourth iteration of both datasets sketched against *b* and *p*.
In the next part we will demonstrate the best outcome of every iteration with their respecting parameters.

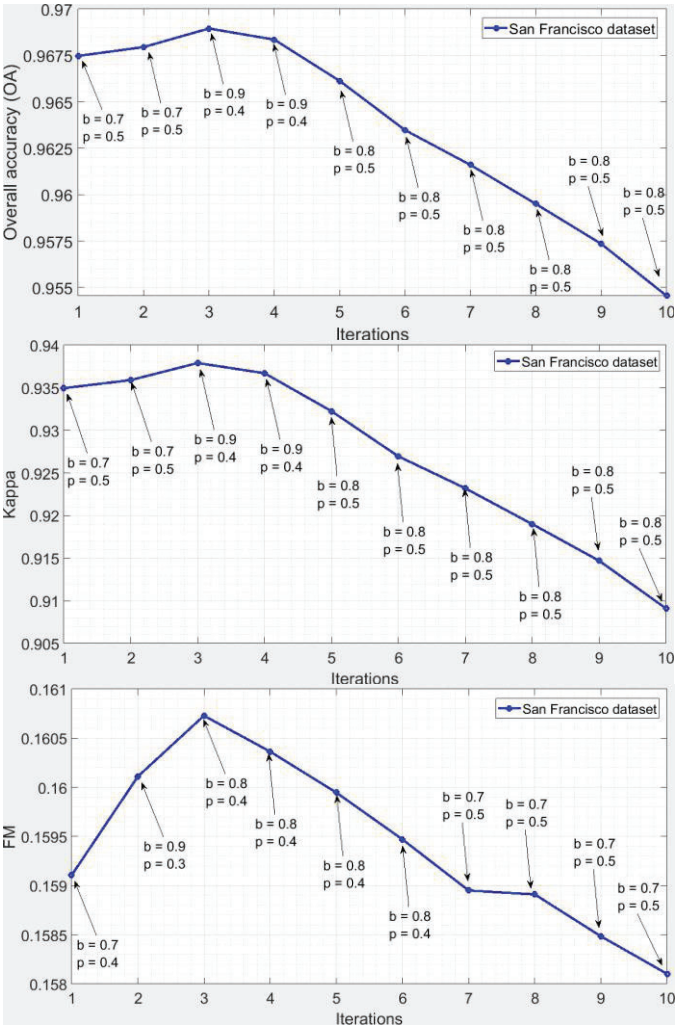

Figure 9: A) best of 3 indexes in each iteration with their respecting parameters

Since maximum or minimum of recall and OE rates is either 0% or 100%, they don't convey information and therefore, only OA, Kappa and FM are plotted in figure 9. It is seen that in Dataset 1 we have achieved better maximum performance in third iteration in all indexes and in dataset 2 better performance in only FM in second iteration.

As it is mentioned before, the best results appear within the first 3 or 4 iterations.

For comparison We will compare the best results of the proposed method (using optimum parameters and iterations) to results from using Erosion and opening operations on the PD output. The structuring element is the smallest plus shaped object.

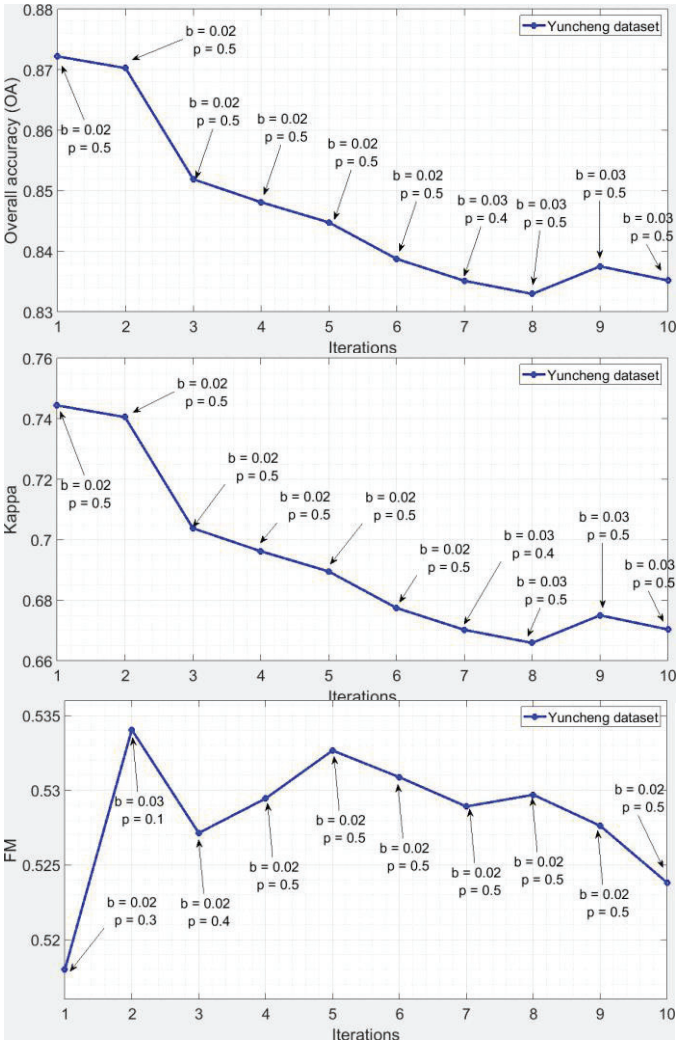

Figure 9: B) best of 3 indexes in each iteration with their respecting parameters

In the tables 1-4 best outcome of the first iterations are compared to HyRes and FORPDN alternatives.

Table 1: dataset 1, performance of proposed method using b = 0.7, p = 0.5 and 2 iterations in comparison

Approach	OA	Kappa	OE	Recall	FM
Erosion	94.95%	89.90%	**4.19%**	**95.81%**	**15.77%**
Opening	**96.94%**	**93.88%**	12.67%	87.33%	14.86%
Proposed method	96.79%	93.59%	10.10%	89.90%	15.21%
PD	96.73%	93.46%	17.01%	82.99%	14.20%

Table 2: dataset 1, performance of proposed method using b = 0.9, p = 0.4 and 3 iterations in comparison

Approach	OA	Kappa	OE	Recall	FM
Erosion	96.09%	92.18%	**12.61%**	**87.39%**	**14.75%**
Opening	96.40%	92.81%	29.30%	70.70%	12.32%
Proposed method	**96.89%**	**93.79%**	17.01%	82.99%	14.22%
PD	95.81%	91.62%	37.30%	62.70%	11.01%

Table 3: dataset 2, performance of proposed method using b = 0.03, p = 0.1 and 2 iterations in comparison

Approach	OA	Kappa	OE	Recall	FM
Erosion	77.84%	55.69%	5.24%	94.76%	49.84%
Opening	84.16%	68.32%	10.18%	89.82%	51.30%
Proposed method	83.83%	67.65%	**1.66%**	**98.34%**	**53.40%**
PD	**85.04%**	**70.08%**	13.15%	86.85%	50.88%

Table 4: dataset 2, performance of proposed method using b = 0.02, p = 0.4 and 3 iterations in comparison

Approach	OA	Kappa	OE	Recall	FM
Erosion	80.39%	60.78%	7.13%	92.87%	50.43%
Opening	85.50%	**87.25%**	12.75%	87.25%	51.21%
Proposed method	82.44%	64.88%	**1.88%**	**98.12%**	**52.71%**
PD	**86.32%**	72.65%	15.92%	84.08%	50.69%

It is demonstrated that the proposed method can improve raw change map produced by percent difference method and compete with alternative methods such as common morphological operations. As mentioned before, fair distance between changed areas leads to better results (San Francisco dataset). Which in some applications such as detection of vehicles (In land or seas), detection of changed areas in urban areas and etc. is present. Even when the condition is not satisfied by any means (Yuncheng Dataset), some indexes indicate better performance such as FM, Recall and OE. Below there are final results with aforementioned parameters. Since a small part of the proposed method is random regarding the parameter (r), it is expected that running the method repeatedly would result in slightly different outcomes. Final results are depicted in figure 10.

Figure 10: A) dataset 1- left: result of proposed method - right: result of Percent difference method with the same parameters- above: b = 0.9, p = 0.4 and 3 iterations - below: b = 0.7, p = 0.5 and 2 iterations

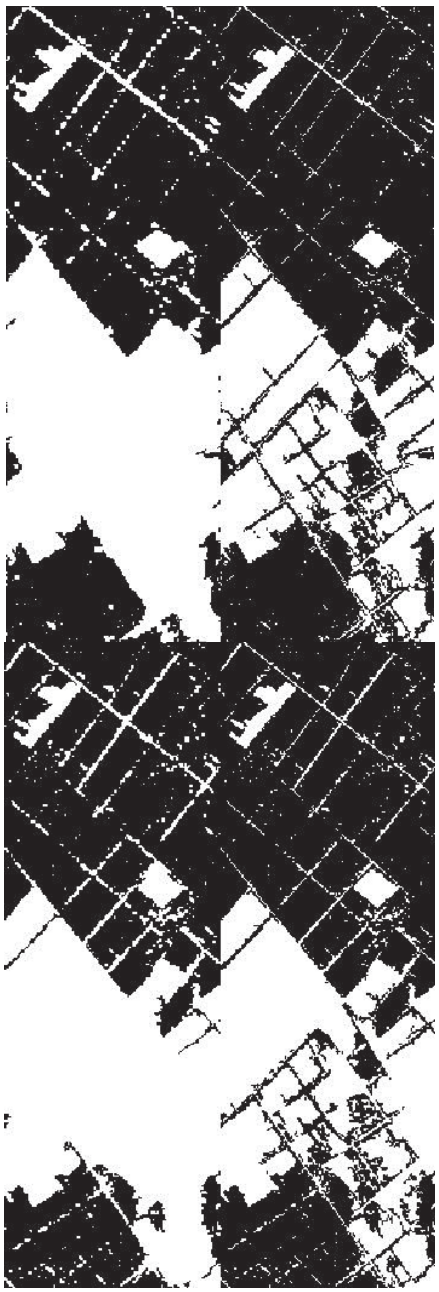

Figure 10: A) dataset 2- left: result of proposed method - right: result of Percent difference method with the same parameters- above: b = 0.02, p = 0.4 and 3 iterations - below: b = 0.03, p = 0.1 and 2 iterations

V. Conclusion and Future Work

In conclusion the proposed method can enhance change maps using well-chosen parameters with low computational cost.

For choosing the proper parameters other algorithms such as Otsu's algorithm can be used. The probability of changing pixels assigned with value of 4 in adjacency map (r) can be optimized; possibly improving performance on the second dataset. Other morphological operations can be used as well.

Other structuring elements may be used for comparison. A number of adaptive algorithms on optimizing the shape of the structuring element might prove to be helpful.

Acknowledgment

I am grateful to have Prof. Pourreza's review on this paper. The datasets were downloaded from website of University of Tehran remote sensing lab...

References

[1] M. İlsever and C. Ünsalan, "Pixel-based change detection methods," in *Two-Dimensional Change Detection Methods*: Springer, 2012, pp. 7-21.

[2] D. Perez, Y. Lu, C. Kwan, Y. Shen, K. Koperski, and J. Li, "Combining satellite images with feature indices for improved change detection," in *2018 9th IEEE Annual Ubiquitous Computing, Electronics & Mobile Communication Conference (UEMCON)*, 2018, pp. 438-444: IEEE.

[3] J. Deng, K. Wang, Y. Deng, and G. Qi, "PCA-based land-use change detection and analysis using multitemporal and multisensor satellite data," *International Journal of Remote Sensing,* vol. 29, no. 16, pp. 4823-4838, 2008.

[4] C. Wu, L. Zhang, and B. Du, "Hyperspectral anomaly change detection with slow feature analysis," *Neurocomputing,* vol. 151, pp. 175-187, 2015.

[5] A. Schaum, "Local covariance equalization of hyperspectral imagery: Advantages and limitations for target detection," in *2005 IEEE Aerospace Conference*, 2005, pp. 2001-2011: IEEE.

[6] J. Zhou, C. Kwan, B. Ayhan, and M. T. Eismann, "A novel cluster kernel RX algorithm for anomaly and change detection using hyperspectral images," *IEEE Transactions on Geoscience and Remote Sensing,* vol. 54, no. 11, pp. 6497-6504, 2016.

[7] J. Zhou, B. Ayhan, C. Kwan, and M. Eismann, "New and Fast algorithms for Anomaly and Change Detection in Hyperspectral images," in *International Symposium on Spectral Sensing Research*, 2010.

[8] N. Jamil, T. M. T. Sembok, and Z. A. Bakar, "Noise removal and enhancement of binary images using morphological operations," in *2008 International Symposium on Information Technology*, 2008, vol. 4, pp. 1-6: IEEE.

[9] K. A. M. Said, A. B. Jambek, and N. Sulaiman, "A study of image processing using morphological opening and closing processes," *International Journal of Control Theory and Applications,* vol. 9, no. 31, pp. 15-21, 2016.

[10] R. Srisha and A. Khan, *Morphological Operations for Image Processing : Understanding and its Applications*. 2013.

[11] P. Salembier, "Structuring element adaptation for morphological filters," *Journal of visual communication and image representation,* vol. 3, no. 2, pp. 115-136, 1992.

[12] A. Song, J. Choi, Y. Han, and Y. Kim, "Change detection in hyperspectral images using recurrent 3D fully convolutional networks," *Remote Sensing,* vol. 10, no. 11, p. 1827, 2018.
[13] Q. Wang, Z. Yuan, Q. Du, and X. Li, "GETNET: A general end-to-end 2-D CNN framework for hyperspectral image change detection," *IEEE Transactions on Geoscience and Remote Sensing,* vol. 57, no. 1, pp. 3-13, 2018.
[14] X. Li, Z. Yuan, and Q. Wang, "Unsupervised deep noise modeling for hyperspectral image change detection," *Remote Sensing,* vol. 11, no. 3, p. 258, 2019.
[15] B. Rasti, P. Scheunders, P. Ghamisi, G. Licciardi, and J. Chanussot, "Noise reduction in hyperspectral imagery: Overview and application," *Remote Sensing,* vol. 10, no. 3, p. 482, 2018.
[16] B. Rasti, P. Ghamisi, and J. Chanussot, "Mixed Noise Reduction in Hyperspectral Imagery," in *2019 10th Workshop on Hyperspectral Imaging and Signal Processing: Evolution in Remote Sensing (WHISPERS)*, 2019, pp. 1-4: IEEE.
[17] C. Aswathy, V. Sowmya, and K. Soman, "Hyperspectral image denoising using low pass sparse banded filter matrix for improved sparsity based classification," *Procedia Computer Science,* vol. 58, pp. 26-33, 2015.
[18] Q. Yuan, Q. Zhang, J. Li, H. Shen, and L. Zhang, "Hyperspectral image denoising employing a spatial–spectral deep residual convolutional neural network," *IEEE Transactions on Geoscience and Remote Sensing,* vol. 57, no. 2, pp. 1205-1218, 2018.
[19] M. T. Eismann, J. Meola, and R. C. Hardie, "Hyperspectral change detection in the presenceof diurnal and seasonal variations," *IEEE Transactions on Geoscience and Remote Sensing,* vol. 46, no. 1, pp. 237-249, 2007.
[20] A. G. Fore *et al.*, "UAVSAR polarimetric calibration," *IEEE Transactions on Geoscience and Remote Sensing,* vol. 53, no. 6, pp. 3481-3491, 2015.
[21] A. Najafi and M. Hasanlou, "Land cover changes detection in polarimetric SAR data using algebra, similarity, and distance based methods," *Engineering Journal of Geospatial Information Technology,* vol. 6, no. 2, pp. 143-163, 2018.
[22] C. Wu, B. Du, and L. Zhang, "A subspace-based change detection method for hyperspectral images," *IEEE Journal of selected topics in applied earth observations and remote sensing,* vol. 6, no. 2, pp. 815-830, 2013.
[23] S. Achour, M. Chikr Elmezouar, N. Taleb, K. Kpalma, and J. Ronsin, "A PCA-PD fusion method for change detection in remote sensing multi temporal images," *Geocarto International,* pp. 1-18, 2020.